Simulation of Positive Corona Discharge in Atmospheric-pressure Air by Plasma Hydrodynamic Model

C. Zogning, J. Lobry and F. Moiny
University of Mons, General Physic Department, Faculty of Engineering, Belgium
Email: calvin.zogning@umons.ac.be

Résumé: Cet article présente les résultats d'une simulation numérique bidimensionnelle axisymétrique dépendante du temps d'une décharge corona positive dans une configuration pointe-plan dans l'air à pression atmosphérique. La simulation a été réalisée à l'aide du module Plasma de COMSOL Multiphysics®. La simulation utilise des espèces plasma-chimique simplifiée et un ensemble de réactions pour l'air à pression atmosphérique, en tenant compte des processus d'ionisation des électrons, de dissociation par impact électronique, d'attachement et de photoionisation dans le gaz. De plus, le coefficient de vitesse des réactions et la photoionisation ont été calculé à l'aide de l'interface PDE. Les résultats de la simulation montrent que le canal de plasma se compose de deux zones : « glow corona » sous forme de jet fin près de l'électrode pointue et le streamer se propageant à partir de la lueur vers l'électrode mise à la terre. Les résultats obtenus sont comparés aux données expérimentales de la littérature et nous constatons qu'ils sont en bon accord.

Abstract: This paper presents the results of a two-dimensional axisymmetric time-dependent numerical simulation of a positive corona discharge in the point-to-plane configuration filled with air at atmospheric pressure. The simulation was carried out using the Plasma module of COMSOL Multiphysics®. The simulation uses a simplified plasma-chemical species and reaction set for air at atmospheric pressure, considering the process of electron ionization, impact dissociation, attachment, and gas photoionization. Additionally, the photoionization rate coefficient was calculated using the PDE interface. The simulation results show that the plasma channel consists of two areas: corona glow in form of thin jet near the tip electrode and streamer propagating from glow corona towards the grounded electrode. The results obtained are compared with the experimental data in the literature and we note that they are in good agreement.

Introduction

The physical understanding of non-equilibrium cold plasmas at atmospheric pressure, at least on small time scales, relies on the concept of highly nonlinear space charges distribution. Streamers are rapidly expanding ionized filaments that can appear in gases, liquids, and solids in the presence of a strong electric field. They are generated by high electric fields but can penetrate areas where the background electric field is below that of the ionization threshold. This is possible because the inside of the streamer channel is made of conductive plasma. Therefore, the electric field in this channel is largely masked [1]. This is only possible when the interior is surrounded by a space charge layer.

The positive corona discharge in the atmospheric air has been the subject of many theoretical studies for several years [2-4,6-12]. However, a complete theoretical description of the development of the discharge still presents some difficulties due not only to the physical mechanisms which are extremely complex for experimental diagnostics and theoretical description, but also to consider the wide range of initial conditions, in which discharge occurs. It is also necessary to note the large number of species and chemical reactions in the plasma of the air discharge, which further complicates the numerical calculation of the gas discharge.

This paper presents the results of a two-dimensional axisymmetric time-dependent numerical simulation of a positive corona discharge in the point-to-plane configuration filled with air at atmospheric pressure. The simulation was carried out based on the hydrodynamic model of the discharge carried out using the COMSOL Multiphysics® Plasma module. The simulation uses a simplified plasma-chemical species and reaction set for air at atmospheric pressure, considering the process of electron ionization, impact dissociation, attachment, and gas photoionization. Additionally, the photoionization rate coefficient was calculated using the PDE interface.

Description of the numerical simulation model

Our simulation is based on the experimental investigation of corona discharge characteristics, carried out in the Institute of High-Current Electronics [13]. A specific feature of the corona discharge is that, for its formation, it sufficient to apply a high voltage to the electrode with small radius of curvature. In this case, the discharge was excited in atmospheric-pressure air between thin high-voltage tip and plane grounded electrode. The corona discharge was observed near the high-voltage tip. Based on the experiment, we build a simplified computational geometry [13]. A three-dimensional experimental configuration was substituted by a two-dimensional axisymmetric configuration. The geometry parameters were taken from the experiment. The width of computational domain must be large enough so that the open boundaries do not affect the plasma channel. The needle has a hyperbolic tip with a radius of curvature equal to 100 µm and is placed 5 mm away and perpendicular to the ground plane. The needle

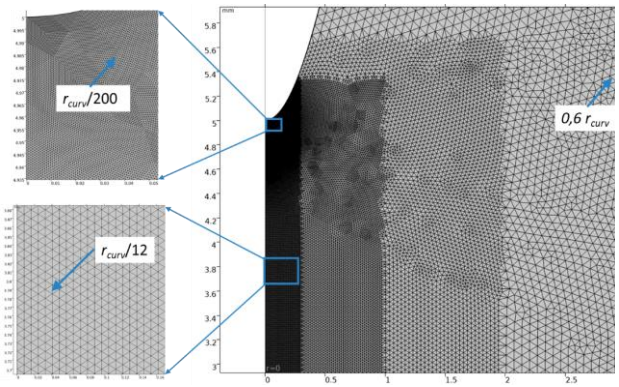

Figure 1. Simulation Geometry and mesh distributions.

electrode is connected to 10 kV dc voltage. The computation domain is a 10 mm × 10 mm rectangle, which is a popular size in the numerical investigations of positive corona discharge [5,6,8].

A physics-controlled mesh is not suitable for the problem of local plasma generation. That is why we applied a user-controlled mesh. To calculate the plasma variables correctly, it is necessary that the mesh size in the entire computation domain be several times smaller than the Debye length. It is also necessary to refine mesh near the tip curvature and the axis of symmetry, where the high plasma density is observed. The geometry and mesh of the computation domain is presented in Figure 1. The number of mesh elements is around 154k, with an average quality of 0.9 and a minimum quality of 0.3. This corresponds to an effective mesh. The number of degrees of freedom is around one million and a simulation time of up to 18 hours. The time steps in the streamer discharge models are determined and fixed by us and must consider the very small mesh along the axis of the discharge. The time step is fixed at 10^{-11}s and justifies the duration of the simulation, however, leads to robustness and greatly reduces errors.

The hydrodynamic approach used in the Plasma Module is a well-established theoretical method for describing a high-pressure gas discharge. The approach describes the plasma as a mixture of electrons and ions, moving one through the other. It can be described using the continuity equations coupled with Poisson's equation for electric field, as shown below [14]:

$$\frac{\partial n_e}{\partial t} - \nabla\left[n_e\mu_e\vec{E} + D_e\nabla n_e\right] = R_e + R_{ph}$$

$$\frac{\partial n_\varepsilon}{\partial t} - \nabla\left[n_\varepsilon\mu_\varepsilon\vec{E} + D_\varepsilon\nabla n_\varepsilon\right] + \vec{E}\cdot\left[n_e\mu_e\vec{E} + D_e\nabla n_e\right] = R_\varepsilon$$

$$\Delta V = \frac{q}{\varepsilon_0}\left(\sum_{k=1}^{N} Z_k\rho\omega_k - n_e\right), \vec{E} = -\nabla V$$

$$\rho\frac{\partial\omega_k}{\partial t} - \nabla\left[\rho\omega_k\overrightarrow{V_k}\right] = R_k$$

where t is time, n_e and n_ε are the electron density and energy density respectively, $D_{e,\varepsilon} = \mu_{e,\varepsilon}T_e$ are the electron diffusivity and electron energy diffusivity respectively, $\mu_{e,\varepsilon}$ are the electron mobility and electron energy mobility respectively, T_e is electron temperature, $\vec{E}$ is the electric field vector, ρ is the mixture density, Z_k, V_k, ω_k are respectively the charge number, the multicomponent diffusion velocity and the mass fraction of k-th species, q is the electric charge, V is the electric potential, ε_0 is the permittivity of vacuum, R_e is either a source or a sink of electrons, R_ε is the energy loss or gain due to inelastic collisions, R_k is the rate expression of k-th species computed using the BOLSIG+ code [15]. Pay attention to the right-hand side of the continuity equations: we've added a photoionization source term.

Photoionization process is described by three linear Helmholtz equations using the Coefficient Form PDE Interface of Mathematics Module:

$$\Delta S_j - \left[\lambda_j p_{O_2}\right]^2 S_j = -A_j p_{O_2}{}^2\frac{0.1p_q}{p+p_q}R_e$$

where p_{O_2} is the partial pressure of molecular oxygen and p_q is quenching pressure, j = 1,2,3, λ_j and A_j are constants defined in [11,12].

The term of photoionization is segregated from the plasma variables. We also used the reaction terms stabilization to avoid approaching zero the electron density values. A complete kinetics of air (excluding any admixtures) includes over 300 reactions. But most of these reactions do not affect the plasma transport properties. For example, the transitions to various exited states, productions of unstable complexes and radicals, and so on. So, our task was to determine the minimal reactions set that allows to correctly describe the development of positive corona discharge. The minimal

Type of reaction	Reaction	Rate expression
Impact ionization	$e+O_2 \Rightarrow 2e+O_2^+$	Townsend coefficients were calculated using the BOLSIG+ code
Impact ionization	$e+N_2 \Rightarrow 2e+N_2^+$	Townsend coefficients were calculated using the BOLSIG+ code
Electron attachment	$O_2+O_2+e \Rightarrow O_2+O_2^-$	$1.9\times10^{-30}.(0.026/T_e).\exp[(1-0.026/T_e).7/3]$
O_4^+ production	$N_2+O_2+O_2^+ \Rightarrow N_2+O_4^+$	2.4×10^{-30}
Three-body recombination	$N_2+O2^-+O_4^+ \Rightarrow 3O_2+N_2$	2.0×10^{-25}
Three-body recombination	$N_2+O_2^-+O_2^+ \Rightarrow 2O_2+N_2$	2.0×10^{-25}
Impact dissociation	$e+O_2^+ \Rightarrow O+O$	$4.2\times10^{-9}.\exp(-5.6/T_e)$
Photoionization	$h\nu + O_2 \Rightarrow e + O_2^+$	Calculated using Helmholtz equation set

Table1. Minimal reactions set (units of two-body reaction rates – cm^3/s, three-bodies – cm^6/s). Electron temperature Te given in eV.

set includes photoionization, electron impact ionization and attachment, O_4^+ production, recombination, and dissociation (see Table 1.) [11, 15-17].

Results and discussions

When subjected to an external electric field, the initial electrons move to the cathode and collide with the molecules in the gas to generate other electrons, as well as positive ions and negative ions, causing the conversion into a streamer. As will be seen in the results, the structure of the plasma channel consists of two areas: a luminescent ionization zone ("glow corona") near the tip electrode, in the form of a thin jet. And a second zone, that of a streamer propagating from the luminescent jet to the cathode, this until a rupture of the gaseous space (breakdown) occurs.

Electric Field Distributions

Figure 2 shows a 2D representation of the spatial distribution of the electric field during streamer development in the tip-plane interval. It can be observed that the electric field is high at the head of the streamer and a strongly reduced field strength in the plasma channel behind the head of the streamer where the electrical conductivity is high. After 10.6 ns, the streamer near the flat electrode causes a sharp increase in the electric field at the head of the streamer, which eventually leads to a breakdown. This reflects the electrostatic interaction between the plasma channel with a certain electrical potential and the grounded electrode. Under the effect of the electric field, the density of electrons resulting from the ionization of gas molecules as well as photoionization gradually increases. The electrons concentrated in the head of the streamer also strengthen the electric field and accentuate the ionization and photoionization processes. Under the effect of the electric field and electron scattering, the streamer gradually develops from the tip electrode to the plane electrode. There are electrons, positive ions, and negative ions in the area where the streamer passes, which further breaks down the background gas.

Electron Number Density Distributions

Figure 3 illustrates the distribution of the densities of electrons, at various times during the development of the streamer. Note that we took the logarithmic form. The position of the maximum electron density also changes with the development of the streamer. At t = 10.6 ns, the electric field between the streamer head and the cathode increases sharply due to the narrowing of the space between the streamer head and the cathode. Therefore, as

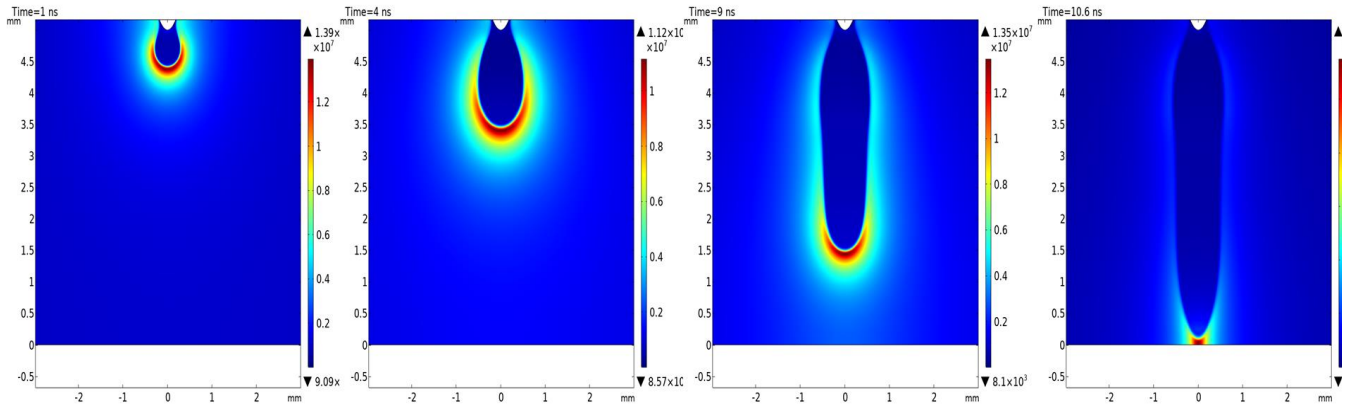

Figure 2. Electric field distribution (V/m) along the plane of the needle from 1 ns to 10.6 ns.

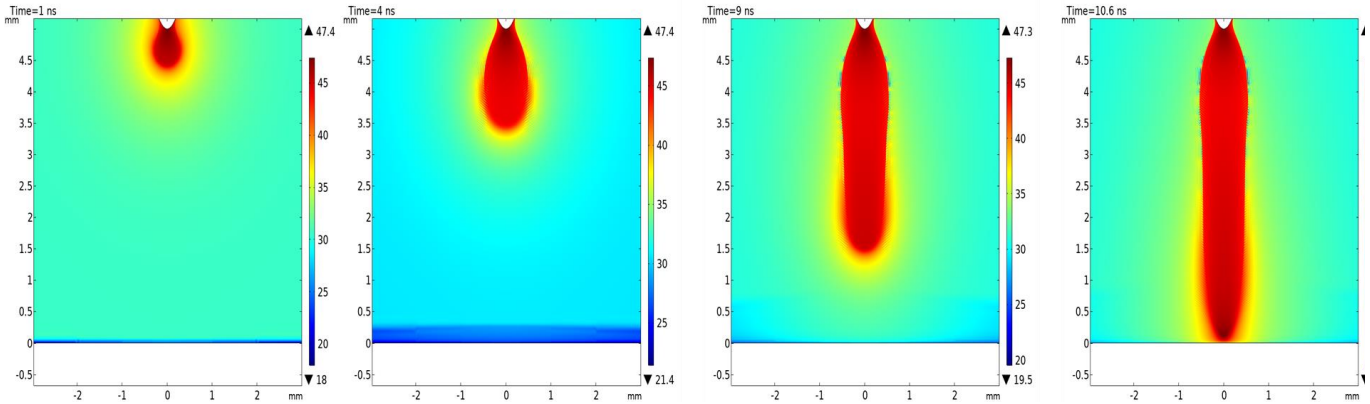

Figure 3. Electron Number Density Distributions along the plane of the needle from 1 ns to 10.6 ns.

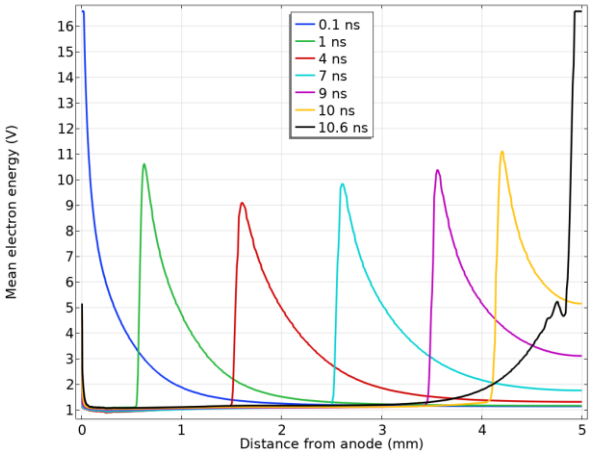

Figure 4. Mean electron energy distribution along the plane of the needle from 0.1 ns to 10.6 ns.

the strength of the electric field increases, the ionization becomes more intense so that electron densities increase to values of 4.0×10^{20} m^{-3}, resulting in a positive glow at the head of the streamer. The streamer finally crosses the inter-electrode space of 5 mm in 10.6 ns, which corresponds to an average frontal speed estimated at about 0.47 mm/ns, which remains in agreement with previous works [9, 10] and is well within the range between 10^5 and 10^7, which is the speed of propagation of streamers in small intervals [8]. The diameter of the streamer channel is measured, and its value is between 0.8 and 1 mm. It can also be calculated from the propagation speed. The results are also consistent with the data in the literature [8].

Electron energy Distribution

Ion impact reactions (ionization and attachment) significantly affect streamer discharge. The collision rates between a molecule and an electron and the transport coefficient of an electron (for example, the diffusion coefficient and the mobility of the electrons) are, in general, functions of the average energy of the electrons. Therefore, research on the energy profile of electrons in the streamer discharge is extremely important for a comprehensive understanding of the physical mechanism. Figures 4. show the axial profile of the mean electron energy. The average electron energy in the streamer channel is about 1 eV, and ranges from 9 to 16 eV at the streamer head. Sigmund et al. [3] estimate that when the reduced electric field of the streamer head varies from 400 to 600 Td, the average energy of the electrons in the streamer head varies from 12 to 16 eV. This value is slightly higher than that
reported in our work, with a reduced electric field at the head of the streamer varying from 430 to 600 Td. This is since in our work we use a local field approximation. Then, the electron energy density equation is not solved, and the transport and source coefficients are instead a function of the reduced electric field. In practice, when using local field approximation or local energy approximation, transport and source coefficients are always given as a function of the average electron energy. However, when using the local field approximation, a function that connects the average energy of the electrons and the reduced electric field must be considered.
It can nevertheless be noticed that the ionization processes take place only during the glow discharge (0.1 ns) and when the streamer comes very close to the planar electrode (10.6 ns). At these precise instants the average energy of the electrons is substantially equal to 16.07 eV, sufficiently above the ionization threshold of the nitrogen molecules (15.6 eV) and that of the oxygen molecules (12.07 eV). Moreover, the process of propagation of the streamer is governed by photoionization since the electrons no longer have enough energy to ionize the gas.

Photoionization and electron impact ionization rate Distribution

As mentioned before, photoionization plays a primary role in the propagation of streamers. The photoionization reaction in air is a process in which oxygen molecules absorb the light emitted by excited nitrogen molecules,

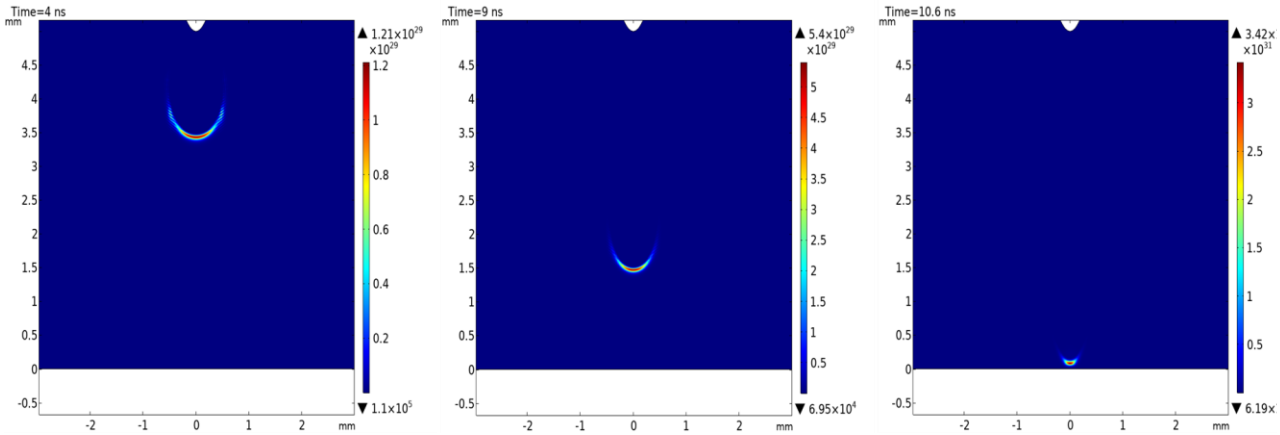

Figure 5. Electron impact ionization rate Distribution (1/(m^3.s)) along the plane of the needle from 4 ns to 10.6 ns.

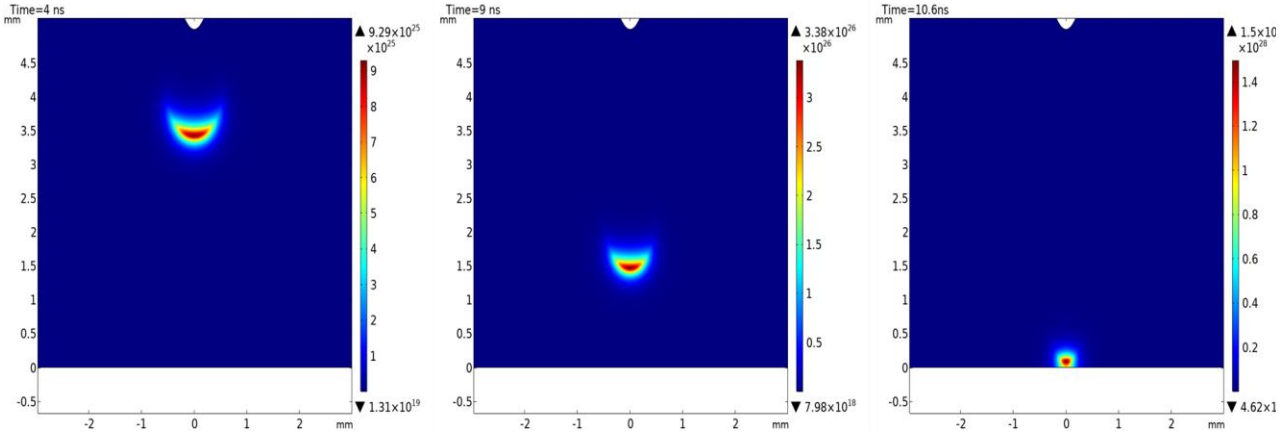

Figure 6. Photoionization rate Distribution (1/(m^3.s)) along the plane of the needle from 4 ns to 10.6 ns.

leading to ionization. Since photoionization occurs in a wider range than electron impact ionization, electrons can be generated in a region slightly farther from the electrode and streamer head. Figures 5 and 6 show the spatial distributions of photoionization and electron impact ionization reactions during streamer development. In Figure 6, electron impact ionization mainly occurs near the high electric field region around the streamer head (see figure) and hardly occurs in the low electric field region in the streamer channel and in the area away from the streamer head. The photoionization rate propagates spherically around the head of the streamer and in a wider range than the electron impact ionization rate. Comparing Figures 5 and 6, it can be noted that electron impact ionization has a locally high ionization rate but in a narrow range, while photoionization has a low ionization rate but in a wide range.

Conclusion

In summary, we developed the theoretical model of positive corona discharge in atmospheric-pressure air. The simulation results show that the plasma channel consists of two areas: corona glow in form of thin jet near the tip electrode and streamer propagating from glow corona towards the grounded electrode. We developed the minimal reaction set in air, which includes electron attachment, impact dissociation, photoionization and so on, which correctly describes the breakdown development. We compared the simulation results with experimental data and obtained good agreement.

Acknowledgment

This work has been supported by Université de Mons. The author is grateful to the University of Mons for allowing them to carry out their research work.

References

[1] P. Dordizadeh, K. Adamiak and GSP. Castle J Electrost 84:73–80, (2016).

[2] G. G. Hudson and L. B. Loeb, “Streamer mechanism and main stroke in the filamentary spark breakdown in air as revealed by photomultipliers and fast oscilloscopic techniques,” Physical Review 123(1), 29 (1961).

[3] R. S. Sigmond, “The residual streamer channel: Return strokes and secondary streamers,” Journal of Applied Physics 56(5), 1355–1370 (1984).

[4] N. Y. Babaeva and G. V. Naidis, “Two-dimensional modelling of positive streamer dynamics in non-uniform electric fields in air,” Journal of Physics D: Applied Physics **29**, 2423–2431 (1996).

[5] R. Morrow, “Theory of negative corona in oxygen,” Phys. Rev. A Gen. Phys., vol. 32, no. 3, pp. 1799–1809, Sep. 1985. (2005) 722–733.

[6] J. Hui, Z. Guan, L. Wang, and Q. Li, "Variation of the Dynamics of Positive Streamer with Pressure and Humidity in Air," in IEEE.

[7] M. Talaat, A. El-Zein, and A. Samir, “Numerical and simulation model of the streamer inception at atmospheric pressure under the effect of a non-uniform electric field,” Vacuum **160**, 197–204 (2019).

[8] T M P Briels, E M van Veldhuizen, and U Ebert. Positive streamers in air and nitrogen of varying density : experiments on similarity laws. Journal of Physics D : Applied Physics, 41(23) :234008, nov 2008.

[9] A. A Dubinova. Modeling of streamer discharges near dielectrics. PhD thesis, Technische Universiteit Eindhoven, 2016.

[10] Shailendra Singh. Computational framework for studying charge transport in high-voltage gas-insulated systems. PhD thesis, CHALMERS UNIVERSITY OF TECHNOLOGY, 2015.

[11] A. Bourdon, V.P. Pasko, N.Y. Liu, S. Célestin , P. Ségur, and E. Marode, “Efficient models for photoionization produced by non-thermal gas discharge in air based on radiative transfer and the Helmholtz equations,” Plasma Sources Science and Technology, vol. 16, pp. 656-678, 2007.

[12] A. Luque et al Photoionization in negative streamers: fast computations and two propagation modes Appl. Phys. Lett. 90 081501, 2007.

[13] Tarasenko, V.F., Baksht, E.Kh. // Plasma Physics Reports. 44(5), pp. 520-532 (2018).

[14] Young, F.F., Wu, C.H. // IEEE Trans. on Plas. Sci., 21(3), pp. 312–321 (1993).

[15 G.J.M. Hagelaar and L.C. Pitchford, "Solving the Boltzmann equation to obtain electron transport coefficients and rate coefficients for fluid models", Plasma Sci Sources and Tech 14, 722 (2005).

[16] Pancheshnyi et al., “Development of a cathode-directed streamer” Phys. Rev. E, 71, (2005).

[17] He et al., “Modeling Study on the Generation of Reactive Oxygen”, Plas. Proc. and Pol., 9, (2012).